2nd Conference on Production Systems and Logistics

Analysis of surface quality during milling with industrial robots as a function of milling spindle orientation

Lars Niklas Penczek[1], Michael Krampe[1], Bernd Kuhlenkötter[1]

[1] Ruhr University Bochum, Chair of Production Systems, Bochum, Germany

Abstract

The range of tasks performed by industrial robots has become increasingly comprehensive in recent decades. This includes pick-and-place tasks with low to medium handling weights, as well as material processing tasks with medium to high processing forces. Milling in particular involves high-frequency excitation of the material, which results in vibration phenomena and therefor affects the surface quality of the product. These effects were investigated by milling tests at characteristic positions and in different orientations of the milling spindle, using aluminum. For this purpose, based on an experimental modal analysis, a prediction model of the robot's natural frequencies in dependence of the joint positions was developed. This allowed the determination of characteristic milling positions and milling spindle orientations. Subsequently, the milling results were related to a causal connection and were analyzed regarding the natural frequencies.

Keywords

Industrial Robotics; Milling; Tool Orientation; Vibration Analysis; Experimental Modal Analysis; Ball-End Milling Cutter; Regression Model

1. Introduction

The application areas for industrial robots now extend far beyond the classic welding, assembly and bonding tasks. For example, industrial robots are increasingly being used in metalworking applications, such as polishing [1], sheet metal forming [2], deburring, cutting, drilling, grinding and milling. In contrast to CNC machines, articulated robots offer high flexibility, low investment cost per cubic meter of workspace, as well as possible interaction with other machines or additional axes [3]. The machining forces in robots are in a medium to high range, which can lead to a high displacement of the end effector [4] as well as vibration phenomena [5], occurring due to the up to 50 times lower stiffness compared to CNC machines [6]. Especially the milling of hard materials such as metals or ceramics therefor is a great challenge.

The inaccuracies in milling with industrial robots originate in the mechanics, the drives, the programming, the workpiece, the process and the tool. The geometric errors (zero position error, arm length and angle errors) have the greatest influence on the dimensional accuracy and the surface quality of the milled components [7]. Especially the surface quality of the workpieces depends on the vibration phenomena resulting from the excitation of the system and the natural frequencies and modes. Redundant robot poses can be used to influence this effect. The use of ball-end milling cutters makes it possible to extend this redundancy enormously, since the orientation of the milling spindle can be adjusted in all three directions of rotation. This potential will be systematically investigated for the first time in this paper, using a prediction

publish-Ing.

model to determine the natural frequencies. The influence of self-excited vibrations on the milling pattern was investigated in milling tests during finishing.

2. Milling with industrial robots

Nowadays, industrial robots are used in industrial applications and in the cultural industry for the machining of plastic, hard foam, wood and occasionally aluminum parts, where primarily parts with medium quality are milled. Especially for demanding parts with complicated free-form surfaces, jointed-arm robots offer significant advantages in terms of accessibility. The process of milling is basically divided into the machining steps roughing and finishing. During roughing, the chip removal is very large, which means that the process forces that occur and the displacement of the tool center point (TCP) are also particularly high. In finishing, the component is finely machined and high-quality surfaces with narrow tolerances are milled [8], so that any possible surface defects caused by vibrations, are immediately visible in the finished workpiece. In form milling, a spherical cutter is often used in the finishing process, which has a variable approach of the cutter to the surface and thus allows a high number of possible joint configurations.

Robots are particularly susceptible to vibration, because the stiffness for a six-axis industrial robot is typically less than 1 N/µm, while standard CNC machines often have a stiffness of more than 50 N/µm [6]. The vibrations occurring during the milling process can be divided into self-excited and externally excited vibrations. Externally excited vibrations are caused by a multi-bladed tool that is not continuously engaged and thus exerts a periodic force on the robot [9]. In this case the vibration frequency is determined by the excitation frequency. If this frequency is in close proximity to the natural frequencies of the robot, which are usually in the range of about 10 Hz [6], an upswing of the system can be triggered. Therefore, in order to describe the vibration effects comprehensively, a consideration of the excitation frequencies is also useful and will be investigated in more detail in future work.

Among the self-excited oscillations, those resulting from the dynamic process itself and the energy of the robot system's drives, are particularly problematic. Even if no natural frequencies of the system are directly excited by the periodic application of force, the robot still oscillates in its natural frequencies. This leads to wavy contours on the surface of the material, so-called chatter marks. The undulating surface further amplifies this effect for each chip, resulting in self-exciting oscillations.

Both types of vibrations mentioned above are summarized as chatter vibrations in literature. Chatter vibrations do not only reduce the quality of the workpiece, they also drastically increase the load on the tool and milling robot. In unfavorable cases, this can result in damage to the workpiece, tool or robot [10].

3. Model for natural frequency determination in a defined workspace

In order to understand the mechanical oscillation of a robot during milling, the corresponding influencing variables must be determined over the entire workspace. These influencing variables are the natural frequencies of the robot, the excitation frequencies and the milling forces that occur. The natural frequencies vary, depending on the joint position of the robot. In order to determine these natural frequencies, an experimental modal analysis was carried out at characteristic points and a regression model was then created to extend the results over the entire workspace.

Experimental modal analysis (EMA), is the most common method for characterizing the dynamic behavior of mechanical structures. It is built on the foundation of calculating the transfer function $G(\omega)$, which represents the sought linear relationship between the input and output signals of a system in the frequency domain. This function is calculated from the quotient of the excitation spectrum $U(\omega)$ and the resulting

system response $Y(\omega)$. The applied excitation force leads to a structural response, which is measured as acceleration amplitude. This excitation force can be triggered continuously by an electrodynamic excite or impulsively by a hammer blow with force pulse measurement [11].

In order to investigate the natural frequencies, a statistical design of experiments was used. In these experiments specific robot configurations were investigated [12,5], which in the context of this modal analysis, were limited to a working range that can be used for the milling process. A centrally composed experimental design was applied, based on a fully factorial experimental design [13]. The nonlinear relationships between the natural frequencies were investigated by adding star and center points. The orthogonal, centrally composed experimental design now results in a factor level combination table for four factors with three factor levels each. Thus, the number of measurements to be investigated could be limited to a total of 27 joint configurations.
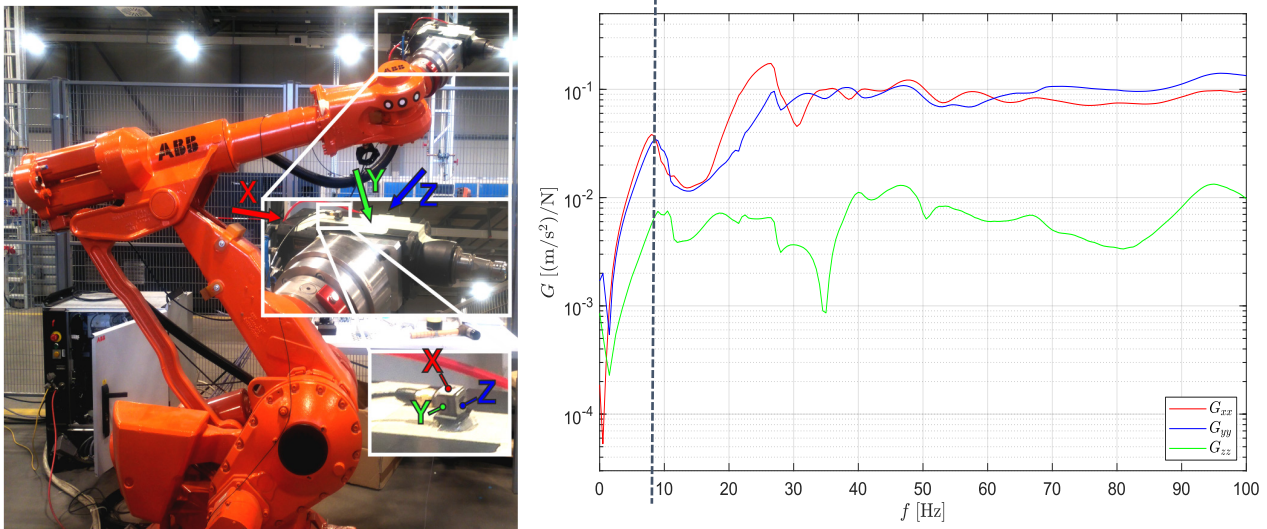

Figure 1: Joint position of the ABB IRB 4400 (left; with force excitation direction) and transmission functions G_{xx}, G_{yy} and G_{zz} as a result of the EMA (right) with the joint configuration: $p_1 = 10, p_2 = 40, p_3 = -15, \ p_4 = -50, \ p_5 = -45, \ p_6 = 0$

The modal analysis was carried out on the *ABB IRB 4400* six-axis robot, which has additional stiffening of the second link in its design, resulting in a particularly positive effect on milling tasks. The heavy-duty impulse hammer Type 8208 from *Brüel & Kjaer* was used to excite the robot, which generates an excitation force of up to 44.4 kN and guarantees a resolution of 0.225 mV/N. The triaxial accelerometer Type 4524-B-001 from *Brüel & Kjaer*, possessing a sensitivity of 10 mV/g, was used to record the resulting systemic response. The system was excited at one measuring point in each of the three coordinate directions, using the single impact method directly on the milling spindle, see Figure 1. The triaxial acceleration sensor was also placed close to the milling spindle, in order to be able to measure the frequencies as close as possible to the TCP.

As already mentioned, a natural frequency in the range of approximately 10 Hz is to be expected, therefore the recording range was set to 0 - 100 Hz. The transfer function was calculated by averaging the measurement results from 5 measurement processes. These measurements showed that the natural frequencies of the robot ranged from 8.4 Hz to 17.9 Hz.

In order to transfer the natural frequencies to the entire workspace and to all poses of the robot, a regression model was developed. From previous investigations in six-axis robots [14] it is known that joints 1 and 6 only have a very small influence on the natural frequency of the robot, compared to other joints. Therefore, they can be neglected for further consideration, so that only the effects of joints 2, 3, 4 and 5 were considered in the model design. The natural frequencies of the robot exhibit a strong nonlinear dependence on the joint

configurations [13], therefore a quadratic model was used to empirically describe the relationship between the target variable y_i and the factors x_1, x_2, x_3 and x_4. For this purpose, the target variable is described by the following term:

$$\vec{y} = \underline{X} \cdot \vec{\beta} \tag{1}$$

where $\vec{y} = [y_1 \quad y_2 \quad \cdots \quad y_n]^T$ as well as $\vec{\beta} = [\beta_{44} \quad \beta_{34} \quad \beta_{33} \quad \beta_{24} \quad \cdots \quad \beta_0]^T$.

Also applies

$$\underline{X} = \begin{bmatrix} x_{41}^2 & x_{41} \cdot x_{31} & \cdots & 1 \\ x_{42}^2 & x_{42} \cdot x_{32} & \cdots & 1 \\ \vdots & \vdots & \vdots & \vdots \\ x_{4n}^2 & x_{4n} \cdot x_{3n} & \cdots & 1 \end{bmatrix}. \tag{2}$$

Therefor

$$y_i = f(x_{4i}, x_{3i}, x_{2i}, x_{1i}, \vec{\beta}) = [x_{4i}^2 \quad x_{4i} \cdot x_{3i} \quad \cdots \quad 1] \cdot \vec{\beta}. \tag{3}$$

Here $\vec{x_i} = [x_{1i} \quad x_{2i} \quad x_{3i} \quad x_{4i}]^T$ denotes the joint variables $[q_2 \quad q_3 \quad q_4 \quad q_5]^T$ from the i-th joint configuration and y_i corresponds to the associated natural frequency. The function $f(\vec{x_i}, \vec{\beta})$ now depends on the parameter vector $\vec{\beta}$ which can be estimated by using the method of the smallest squares [15]. In the method of the smallest squares, the parameter vector $\vec{\beta}$ is defined to minimize the sum of squared errors. This results in

$$\min_{\vec{\beta}} J[f(\vec{x}, \vec{\beta})] = \sum_{i=1}^{n} [y_i - f(\vec{x_i}, \vec{\beta})]^2 \tag{4}$$

If the quality functional $J[f(\vec{x}, \vec{\beta})]$ is derived according to parameter vector $\vec{\beta}$. The result is

$$\frac{dJ}{d\vec{\beta}} = -2\underline{X}^T \vec{y} + 2\underline{X}^T \underline{X} \vec{\beta} \tag{5}$$

For the local and global minimum of the quality functional applies $\frac{dJ}{d\vec{\beta}} = 0$.

This results in [15]

$$\vec{\beta} = (\underline{X}^T \underline{X})^{-1} \underline{X}^T \cdot \vec{y}. \tag{6}$$

In this calculation, the Hessian matrix $\frac{d^2 J}{d\vec{\beta}^2} = 2\underline{X}^T \underline{X}$ is always positively defined, providing the optimal result for the calculated parameter vector $\vec{\beta}$.
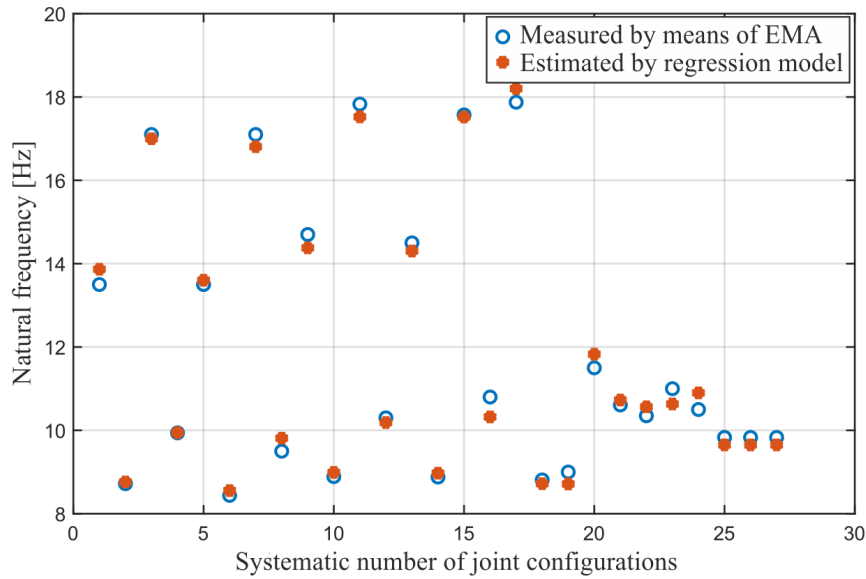
Figure 2: Comparison of the determined natural frequencies between EMA and regression model in different joint configurations

To validate the predictive model, it was compared with a total of 15 points from the real measurement. Figure 2 compares the natural frequencies calculated from the regression model with the results from the EMA. A mean relative error of 3.62% can be observed, allowing a sufficiently good prediction. Thus, a prediction of the natural frequency related to the poses of the robot for the defined milling workspace can be predicted with sufficient accuracy.

4. Results

In order to investigate the effects of the frequency shift, caused by changing the positioning of the milled part and the orientation of the milling spindle, on the surface quality and displacement of the tool, milling tests were run as part of this paper. In addition, the dependence of the milling quality on the milling direction was investigated. Milling on a workspace plane with medium height is expected to be least susceptible to vibrations [16], therefore the investigation of the natural frequencies was limited to a workspace plane at the height of 730 mm. Here, local minima and maxima of the natural frequency were searched for, at milling positions that can be reached by the robot without any problems and that do not lead to collisions with the environment.
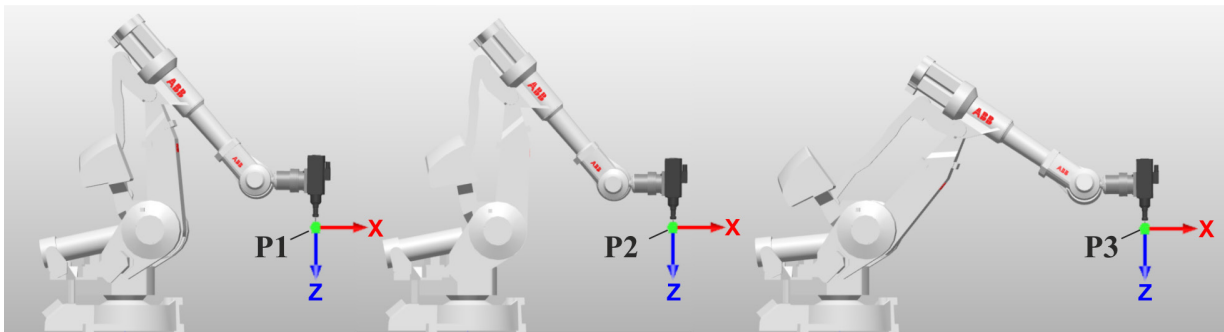

Figure 3: Milling positions in retracted to extended pose (P1: $f = 14{,}4\ Hz, q_2 = -1{,}6°, q_3 = 49{,}0°, q_4 = -4{,}2°, q_5 = -49{,}7°$; P2: $f = 13{,}7\ Hz, q_2 = 5{,}7°, q_3 = 49{,}6°, q_4 = 2{,}5°, q_5 = -48{,}0°$; P3: $f = 10{,}4\ Hz, q_2 = 42{,}4°, q_3 = 33{,}7°, q_4 = -9{,}4°, q_5 = -33{,}0°$)

Accordingly, three milling positions, with orthogonal orientation of the milling spindle to the workpiece surface, posessing a low, medium and high natural frequency were selected; see Figure 3. All milling tests were carried out with a double-edged ball-end cutter with d = 10 mm diameter, since this allows the highest flexibility in terms of redundant robot positions and tool orientations. Subsequently, milling tests were carried out in position P2 (see Figure 3) with different milling spindle orientations. The milling forces were recorded by the *AIT Omega* force-torque sensor. The milling tests were carried out in an aluminum alloy (AlCuMgPb), with the feed rate set to 5 mm/s and a spindle speed of 6,000 rpm.

4.1 Dependency of the milling pattern on the feed direction

In order to investigate the milling pattern in dependence of the feed direction, a star-shaped milling pattern consisting of a total of twelve pockets with identical dimensions was created. These pockets were milled 60 mm long and 10 mm wide. The milling process started in the center of the workpiece surface and ended at the outer end of each pocket at a depth of 6 mm.
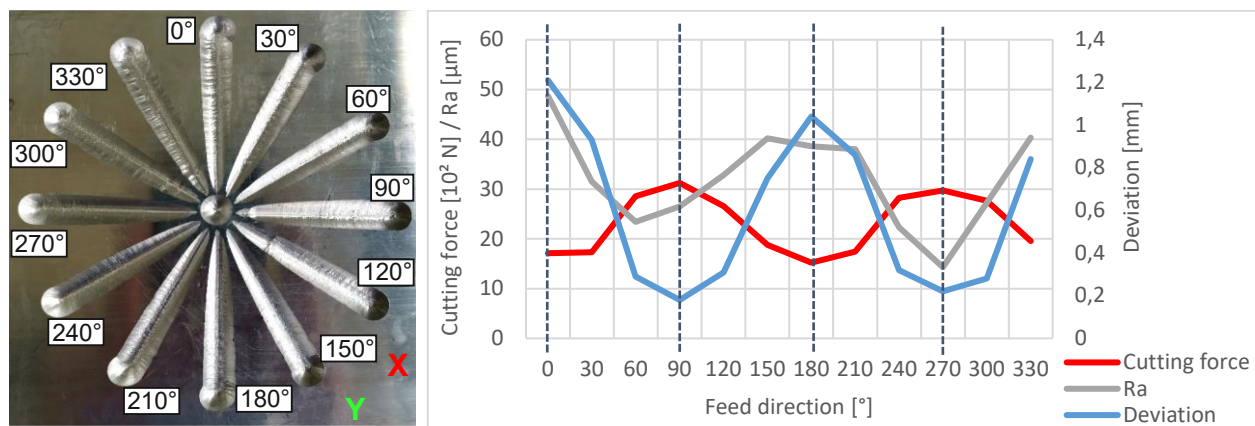

Figure 4: Milling pattern (left) and measured values and milling patterns at position P2 in different feed directions (right)

As expected [16,17], a displacement of the TCP in the rotational direction of the tool was observed; see Figure 4. A significantly lower displacement in feed directions near the y-axes can be seen, whereas the displacement reaches its maximum in the x-axis. This can be explained by the higher section modulus of axes 2, 3 and 5 in the y-direction and the correspondingly acting force direction acting on the robot structure.

As can be seen in Figure 4, this observation is also reflected in the measured milling forces, which are reciprocally proportional to the tool displacement. Due to the higher stiffness of the robot arm when milling in y-direction, higher forces can be applied by the robot, thus reducing tool displacement and improving surface quality. Therefore, the average roughness value R_a in y-direction are about 50% lower than in x-direction.

The milling pattern was carried out at positions P1, P2 and P3, and it was possible to demonstrate correspondingly identical milling behavior in dependence of the feed direction. Thus, a feed in the y direction is clearly preferable to a feed in the x direction. In practice, milling in the y direction cannot always be realized because collisions can occur. Here, a y near milling direction would be conceivable. Furthermore, by using additional axes, an optimization of the milling direction can be realized by the resulting redundant axis configurations in the form of repositioning or reorientation of the robot or the workpiece.

4.2 Dependency of the milling pattern on the position of the milling head

In order to determine the position dependency of the milling results, further milling tests were carried out on the basic poses shown in Figure 3, using the pattern mentioned above. For this purpose, the workpiece was

placed at the different positions and the milling tests were carried out with an orientation of the milling spindle orthogonal to the workpiece surface.
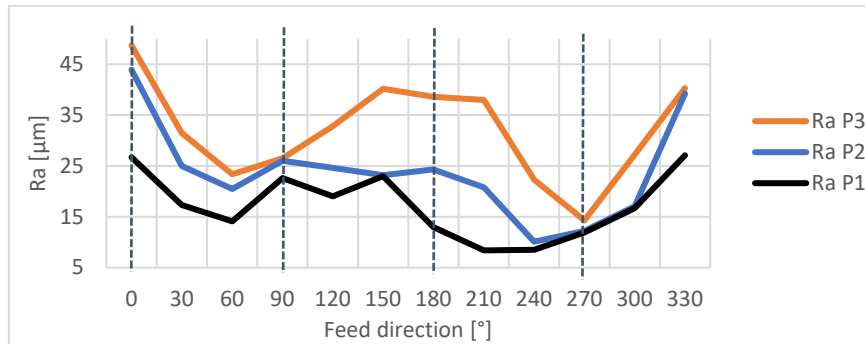

Figure 5: Average roughness value in dependence of the feed direction in the three characteristic positions P1, P2 and P3

Analogous to the milling test in position P2, a parallel sequence of the milling quality in dependence of the feed direction is visible in the two other positions. Nevertheless, a difference in quality can be observed between the individual milling positions. The mean level of the average roughness value R_a changes depending on the position of the robot and the resulting natural frequency. Thus, it can be seen in Figure 5 that R_a averaged over all feed directions is smallest at P1 with 19.5 μm, in the middle range at P2 with 21.3 μm and largest at P3 with 24.2 μm. The natural frequencies therefor are behaving reciprocally proportional to R_a. As expected, the displacement of the TCP and the occurring forces also shift with the poses, depending on the natural frequencies. When milling in y-direction, the values for the milling forces are very high and the R_a-values are quite low, whereas these values are reciprocally proportional during milling in x-direction. Thus, a correlation between higher natural frequencies, which are depending on the axis configurations, and a worse milling pattern can be seen, while milling with a constant orientation of the milling spindle.

4.3 Dependence of the milling pattern on the orientation of the milling head

As mentioned earlier, a ball-end cutter was used in the experiments, which allows a reorientation in the workpiece surface, while maintaining the same profile shape. This allows a great freedom to make use of the redundancy of the robot, since the orientation of the TCP can be varied. The influence of the different orientations on the milling pattern was tested based on the model in position P2.

The test setup allows a reorientation of up to $\pm30°$ in all directions, starting from the initial position P2 shown in Figure 3. The analysis of the milling process in the regression model carried out at the beginning, showed that a reorientation around the RX axis has hardly any influence on the natural frequency. This can be explained by the fact that it is mainly axes 1, 4 and 6 that change here, which have a particularly small influence on the extension of the robot arm. Reorientation around the RZ axis, on the other hand, resulted in a significantly higher change in the natural frequency, since this primarily causes changes in axes 2 and 3. Reorientation around the RY axis had the greatest influence on the natural frequency, since in this case axes 2, 3 and 5 are reoriented primarily, which have a very large influence on the extension of the robot arm. These influences of the change in orientation on the natural frequency were visualized in Figure 6 as an example for one position, based on the regression model. Figure 6 shows possible orientations of the milling spindle with the resulting natural frequency of the robot for this pose. Each orientation of a vector equals the orientation of the milling spindle and the color of the vector equals the natural frequency of the robot. The reorientation results in many redundant poses for the respective orientations, therefore only the respective maximum and minimum natural frequencies were visualized for illustration purposes.
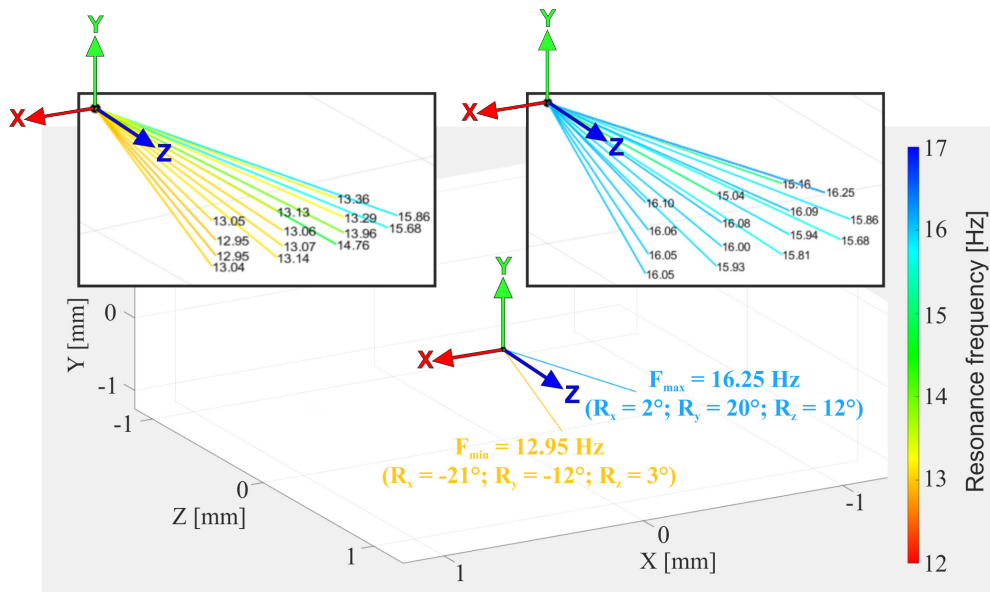
Figure 6: Representation of the reorientation of the milling spindle by ±30° (starting from a TCP zero position of RX = 0, RY = 0, RZ = 0; see position P2) at the pose with the absolute minimum and maximum natural frequencies (center) and respective maximum (top right) and minimum (top left) natural frequencies at the corresponding orientation positions

In order to make this effect of the changed natural frequency as clearly visible as possible in the milling image, milling tests were carried out at position P2 with a reorientation around the RY axis. This reorientation included angles of -30° to +30° starting from the initial position, as shown in Figure 7.

The milling tests were carried out several times and revealed an explicit change in the R_a-values in dependence of the orientation. With the orientation of -30°, where the robot takes up a small extension of the robot arm, a significantly higher average roughness value, than with the orientation +30° can be seen. The best R_a-values could be detected at an orientation of +20° and the worst at -20°.
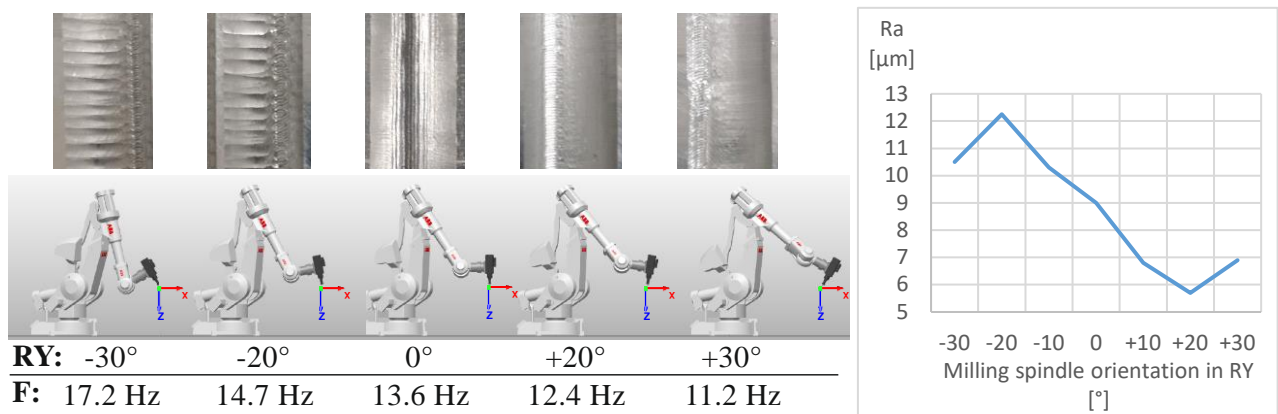

Figure 7: Milling results (left) and R_a-values (right) when reorienting the milling spindle around RY in P2

Contrary to the expectations based on the regression model, a reciprocal proportional relationship between the natural frequencies and the R_a-values cannot be directly proven here. This could be due to various factors influencing the vibration behavior, which have not been considered so far. Among other things, the direction of the force acting during the milling process could play a role, since milling in the direction of or against the robot base results in an opposing load on the motors and joints. Another major influence could be the superposition of the excitation frequencies with the natural frequencies; this effect is to be investigated in more detail in a further paper. It should also be mentioned that due to the design of the ABB IRB 4400, so

due to the multi-point suspension of the amplification of the second link, there is an orientation-dependent change in the section modulus and a change in the position of the balance weight. In order to be able to make a statement about the influence of these factors, further investigations will be necessary in the future. However, the milling tests carried out showed a strong dependence of the milling pattern on the orientation of the milling spindle.

5. Conclusion

The high process forces and high-frequency excitation during milling with robots have the effect of displacing the TCP and forming chatter marks, which is still a challenge. Subject to this problem is the low stiffness of the robot and the resulting oscillation in its natural frequencies. The natural frequencies change with the pose of the robot and in this paper could be determined via experimental modal analysis and transmitted to a regression model in order to be assignable to the entire workspace. Experimentally, during the investigations on an ABB IRB 4400, the basic natural frequency was measured in the range of 8.4 Hz to 17.9 Hz. A correlation of the natural frequencies and the milling position was demonstrated in milling tests and a clear advantage of the feed direction in the y-axis was identified. In addition, the effects of the orientation of the milling spindle on the natural frequencies of the robot and on the milling pattern were investigated. Here, a strong dependence of the surface finish on the orientation of the milling spindle could be demonstrated, but not in a causal relationship to the natural frequencies. In order to better understand the existing vibration phenomena depending on the orientation of the milling spindle, further investigations must be carried out and parameters such as the excitation frequencies, the effect of the additional amplification in link 2, and the direction of force must be included in the evaluation.

References

[1] Plyusnina, M., Krewet, C., Rieger, M., Bickendorf, J., Kuhlenkötter, B. (Eds.), 2015. In-Prozess-Erfassung und Auswertung prozessdefinierender Kennwerte beim robotergestützten Polieren von Designoberflächen: Dortmund (12.03.-13.03.2015): Tagungsband. Technische Universität, Dresden, 263-270.

[2] Möllensiep, D., Spörle, F., Störkle, D.D., Thyssen, L., Kuhlenkötter, B., 2019. Robot-based incremental sheet forming to meet current and future automotive industry requirements: Ideen Form geben, 33. Aachener Stahlkolloquium Umformtechnik, 1. Auflage ed. Verlagshaus Mainz GmbH Aachen, Aachen, 379-388.

[3] Trommer, G., 2009. Standardschnittstelle zur Integration von Maschine und Roboter: Einträgliche Symbiose (6), 58–61.

[4] Abele, E., Bauer, J., Stelzer, M., Stryk, O., 2008. Wechselwirkungen von Fräsprozess und Maschinenstruktur am Beispiel des Industrieroboters: Entwicklung von Modellkomponenten für eine Offlinekompensation der spanenden Bearbeitung mit Industrierobotern. Springer VDI Verlag, 733–737.

[5] Glogowski, P., Kuhlenkötter, B., 2016. Schwingungsanalyse redundanter Roboterportale: Schwingungsminimierung im Fräsbearbeitungsprozess durch optimierte Portalstellungen des Roboters. wt Werkstattstechnik online.

[6] Pan, Z., Zhang, H., Zhu, Z., Wang, J., 2006. Chatter analysis of robotic machining process. Journal of Materials Processing Technology 173 (3), 301–309.

[7] Neto, P., Moreira, A.P. (Eds.), 2013. Robotics in smart manufacturing: International workshop, WRSM 2013; co-located with FAIM 2013, Porto, Portugal, June 26-28, 2013; proceedings. Springer, Berlin, 224 pp.

[8] Paucksch, E., Linß, M., 2008. Zerspantechnik: Prozesse, Werkzeuge, Technologien; Vieweg + Teubner, Wiesbaden, 200 - 212.

[9]   Azeem, A., Feng, H.-Y., Wang, L., 2004. Simplified and efficient calibration of a mechanistic cutting force model for ball-end milling. International Journal of Machine Tools and Manufacture 44 (2-3), 291–298.

[10]   Liu, X., 2009. Machining dynamics: Fundamentals, applications and practices - Machining Dynamics in Milling Processes. Springer, London, 167-231.

[11]   Bertini, L., Neri, P., Santus, C., Guglielmo, A., 2017. Automated Experimental Modal Analysis of Bladed Wheels with an Anthropomorphic Robotic Station. Exp Mech 57 (2), 273–285.

[12]   Bauer, J., 2011. Methoden der Offline-Bahnkorrektur für die spanende Bearbeitung mit Industrierobotern. Zugl.: Darmstadt, Techn. Univ., Diss., 2011. epubli-Verl., Berlin, 32 - 35.

[13]   Basavarajaiah, D. M., Bhamidipati N. M. 2020. Design of experiments and advanced statistical techniques in clinical research , Stringer, Singapore, 100 - 356.

[14]   Glogowski, P., Rieger, M., Kuhlenkötter, B., 2016. Eigenfrequenzbestimmung eines redundanten Roboterportals zur Schwingungsminimierung in Bearbeitungsprozessen, 1 - 12.

[15]   Judge, G.G., Hill, R.C., Griffiths, W.E., Lütkepohl, H., Lee, T.-C., 1988. Introduction to the theory and practice of econometrics, 2. ed. ed. Wiley, New York, 839 - 843.

[16]   Karim, A., Schmid, S., Verl, A., 2017. 24th International Conference on Production research (ICPR 2017): Posnan, Poland, July 30-August 3, 2017. DEStech Publications, Lancaster, 555 - 561.

[17]   Rösch, O., 2015. Steigerung der Arbeitsgenauigkeit bei der Fräsbearbeitung metallischer Werkstoffe mit Industrierobotern. Zugl.: München, Techn. Univ., Fak. für Maschinenwesen, Diss., 2014. Utz, München, 100 - 121.

Biography

Lars Niklas Penczek (*1993), M.Sc. works as a research assistant at the Chair of Production Systems (LPS) at the Ruhr-University Bochum and conducts research in the field of industrial robotics.

Michael Krampe (*1993), M.Sc. works as a research assistant at the Chair of Production Systems (LPS) at the Ruhr-University Bochum and conducts research in the field of industrial robotics.

Till 2009 **Bernd Kuhlenkötter** (*1971) was responsible for product management and technology at ABB Robotics Germany. In 2009 Bernd Kuhlenkötter took over the professorship for "Industrial Robotics and Production Automation" at the Technical University of Dortmund. Since 2015, he holds the professorship of "Production Systems" at the Ruhr-University of Bochum.